

# Relationship between the Pacific and Atlantic stepwise climate change during the 1990s

Y. Chikamoto<sup>1</sup>, M. Kimoto<sup>2</sup>, M. Watanabe<sup>2</sup>, M. Ishii<sup>3,4</sup>, and T. Mochizuki<sup>3</sup>

A linkage between climate change in the Atlantic and the Pacific oceans during the 1990s is investigated using three versions of the coupled climate model MIROC and CMIP5 multi-model ensemble. From the early 1990s to the early 2000s, the observed sea surface temperature (SST) shows warming in the North Atlantic and a La Niña-like pattern in the Pacific. Associated with the SST pattern, the observations indicate a strengthened Walker circulation in the tropical Pacific and enhanced precipitation in the tropical Atlantic. These SST and precipitation patterns are simulated well by hindcast experiments with external forcing and an initialized ocean anomaly state but are poorly simulated by uninitialized simulation with external forcing only. In particular, the observed La Niña-like SST pattern becomes prominent in ensemble members with large amplitudes of Atlantic Multidecadal Oscillation (AMO) index during 1996–1998. Our results suggest that ocean initialization in both the Pacific and the Atlantic plays an important role in predicting the Pacific stepwise climate change during the 1990s, which contributes to the accurate estimation of global temperature change in the coming decade. Forecasting typhoon frequency or marine fisheries production in the coming decade may be possible by improving the predictive skill of stepwise climate change.

## 1. Introduction

A combination of decadal climate variability and the global warming signal occasionally takes a stepwise climate change, sometimes called a climate shift, which has a large impact not only on the regional atmospheric and oceanic variations but also on marine fisheries. In the Pacific, for example, one of the most famous shifts during the mid-1970s was characterized by a phase change of the Pacific Decadal Oscillation (PDO) or the Interdecadal Pacific Oscillation (IPO) [Mantua *et al.*, 1997; Meehl *et al.*, 2009]. Associated with this phase change during the mid-1970s, a coherent shift appeared in the anchovy-sardine population off Japan, California, Chile and Peru, the salmon production for Alaskan stocks, and the groundfish stock in the Northeast Pacific [Mantua and Hare, 2002, and the reference

therein]. During the 1990s, a stepwise shift of Pacific sea surface temperature (SST) was observed [Chikamoto *et al.*, 2012a]. During this period, stepwise shifts also appeared in atmospheric phenomena such as the recent increase in typhoon frequency in Taiwan [Tu *et al.*, 2009], an enhanced summer precipitation in the Korean Peninsula [Kim *et al.*, 2011], and the delayed monsoon onset over the South China Sea [Kajikawa and Wang, 2012].

In addition to these stepwise shifts in the Pacific climate, a rapid SST warming was also reported in the North Atlantic during the mid-1990s [Reverdin, 2010; Robson *et al.*, 2012]. Associated with this SST warming, the Atlantic Multidecadal Oscillation (AMO) showed a rapid phase change from negative to positive [Sutton and Hodson, 2005; Knight *et al.*, 2005]. Specifically, the rapid SST warming in the North Atlantic subpolar gyre region corresponds to 1 K in a 2-year period [Robson *et al.*, 2012]. Recent studies suggest that this rapid SST warming was related to the strengthened Atlantic meridional overturning circulation (AMOC) and a sudden phase change of North Atlantic Oscillation (NAO) [Reverdin, 2010; Robson *et al.*, 2012]. However, it is still unclear whether these abrupt climate changes in the North Atlantic and Pacific are related to each other.

In this study, we examine how the stepwise shift in the North Atlantic affected the Pacific climate shift during the 1990s in hindcast experiments conducted with the MIROC and CMIP5 models. Previous observational and modeling studies have shown that the PDO index on multidecadal timescales was correlated with the AMO index with several years lag [Zhang and Delworth, 2007]. Kucharski *et al.* [2011], using a coupled atmosphere-ocean general circulation model (AOGCM), suggested that the Atlantic SST warming associated with an increase in greenhouse gas concentration induces the La Niña-like response in the Pacific through a strengthened Walker circulation. In addition to this Pacific-Atlantic linkage, recent studies in decadal climate predictability suggest that the PDO, AMO, and stepwise climate changes can be predicted several years in advance by initializing the ocean condition using the AOGCM [Smith *et al.*, 2010; Keenlyside *et al.*, 2008; Mochizuki *et al.*, 2010; Chikamoto *et al.*, 2012a, b]. We will show that the predictability of AMO plays an important role in the simulation of the stepwise shift pattern in the tropical Pacific during the 1990s.

## 2. Model and hindcast experiments

In this study, we use the three versions of AOGCM MIROC: MIROC3m, MIROC4h, MIROC5. In MIROC3m, the atmospheric and oceanic resolutions are a T42 spectral model with 20 levels on vertical  $\sigma$ -coordinates and an approximately  $1^\circ \times 1^\circ$  longitude-latitude grid with 44 vertical levels, respectively. MIROC4h includes the same model physics as MIROC3m but at an eddy-permitting resolution for the ocean: a T213 spectral model with 56 levels in the atmosphere and an approximately  $1/4^\circ \times 1/6^\circ$  longitude-latitude grid with 47 vertical levels in the ocean. In MIROC5, most parts of the model physics are updated or replaced with new parameterization schemes derived from MIROC3m and MIROC4h. The resolution of

<sup>1</sup>International Pacific Research Center, University of Hawaii at Manoa, Honolulu, Hawaii, USA.

<sup>2</sup>Atmosphere and Ocean Research Institute, University of Tokyo, Kashiwa, Chiba, Japan.

<sup>3</sup>Japan Agency for Marine-Earth Science and Technology, Yokohama, Kanagawa, Japan.

<sup>4</sup>Meteorological Research Institute, Tsukuba, Ibaraki, Japan.

## Climate change from 1991/95 to 2000/04

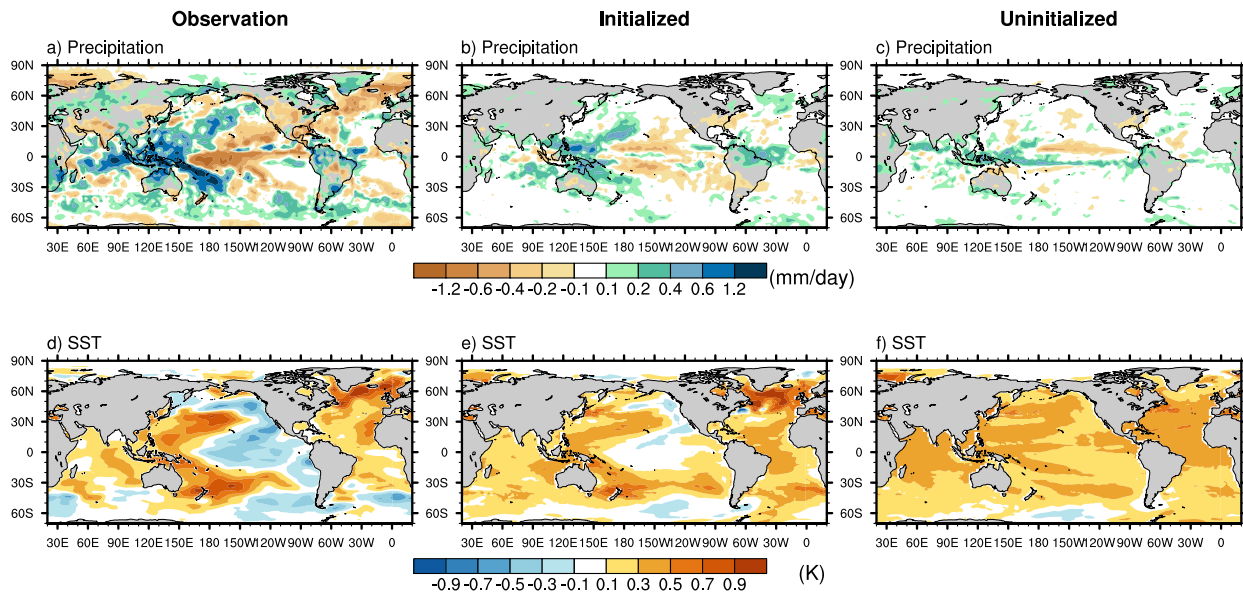


**Figure 1.** Precipitation (upper panels) and SST (lower panels) changes between 1991–95 and 2000–04 in observation and the initialized and uninitialized simulations using the MIROC multi-model. The initialized simulation was obtained from the 2000–04 mean prediction initialized on 1996 and the 1991–05 mean in the assimilation experiment.

MIROC5 is T85 spectral with 40 sigma-pressure hybrid vertical levels in the atmosphere and approximately  $1^\circ$  horizontal grid of curvilinear coordinates with 49 vertical levels in the ocean. Details of the performance and settings of MIROC3m, MIROC4h, and MIROC5 are described in Nozawa *et al.* [2007], Sakamoto *et al.* [2012], and Watanabe *et al.* [2010], respectively.

To evaluate the decadal climate predictability, we conducted the following three experiments using the three versions of MIROC: the 20th century climate simulation (the uninitialized simulation), the data assimilation, and the hindcast experiments (the initialized simulation). In the uninitialized simulation, the model was prescribed by historical natural and anthropogenic forcings, such as greenhouse gases and aerosol concentrations, solar cycle variations, major volcanic eruptions and future emission scenarios based on the CMIP3 and CMIP5 protocols. Using the model climatology defined by the uninitialized simulation, the observed temperature and salinity anomalies in the ocean [Ishii and Kimoto, 2009] were incorporated into model anomalies by an incremental analysis update scheme [Bloom *et al.*, 1996] in the assimilation experiment. The observed temperature and salinity anomalies, obtained from the gridded monthly objective analysis covering the whole ocean produced by Ishii and Kimoto [2009], were linearly interpolated for each day and the ocean model grid. From the assimilation experiment, we can first obtain a pair of atmospheric and oceanic initial conditions and then conduct an ensemble hindcast experiment with a total of 9 hindcasts initialized in 1961, 1966, 1971, 1976, 1981, 1986, 1991, 1996, and 2001 (hereafter, we mainly used the hindcast experiment initialized in 1996). The hindcast experiment has 10, 3, and 6 ensemble members for each of the starting dates in MIROC3m, MIROC4h, and MIROC5, respectively. Details of the model experiment and the assimilation procedure are described in the previous manuscripts [Tatebe *et al.*, 2012; Mochizuki *et al.*, 2012; Chikamoto *et al.*, 2012a, b]. To evaluate the robustness of our results, we also analyze near-term climate prediction experiments in the CMIP5 models. After removing the model drift that arose during prediction from each model, a multi-model ensemble in the initialized simulation is obtained by

averaging over three ensemble means in each model in a similar manner obtained by Chikamoto *et al.* [2012b]. The model drifts in SST and precipitation are estimated on the basis of the assimilation experiment in the MIROC multi-model but of the observation in the CMIP5 models including MIROC5 and MIROC4h. Therefore, precipitation anomalies are obtained in the MIROC models but not in the CMIP5 models because of few observed precipitation datasets covering the entire globe before 1979 owing to the lack of satellite data.

### 3. Results

To examine the model representation of the climate change pattern during the late 1990s, we calculated the SST and precipitation differences between the 1991–95 and 2000–04 means (Fig. 1): the 2000–04 mean minus the 1991–95 mean. In the observation, the SST change shows a warming in the North Atlantic and a La Niña-like pattern in the Pacific (Fig. 1d). Associated with the SST change pattern in the tropical Pacific, a zonal precipitation gradient is observed in the tropical Pacific: a decrease in the central to eastern tropical Pacific and an increase in the western tropical Pacific and the tropical Indian Ocean. This precipitation pattern indicates a strengthened Walker circulation in the Pacific and accompanies enhanced precipitation in the tropical Atlantic. A coherent structure between the strengthened Walker circulation in the Pacific and the enhanced precipitation in the tropical Atlantic is also observed in the divergent wind fields in the troposphere (Fig. S1).

These observed changes in precipitation and SST are represented qualitatively well in the MIROC multi-model of initialized simulation but are not clearly visible in the uninitialized simulation. In the initialized simulation, the SST changes show the La Niña-like pattern in the Pacific and the large warming exceeding 0.9 K in the North Atlantic, particularly, in the North Atlantic subpolar gyre region (Fig. 1e). This simulated SST pattern is consistent with the observation (a pattern correlation coefficient of 0.66), although

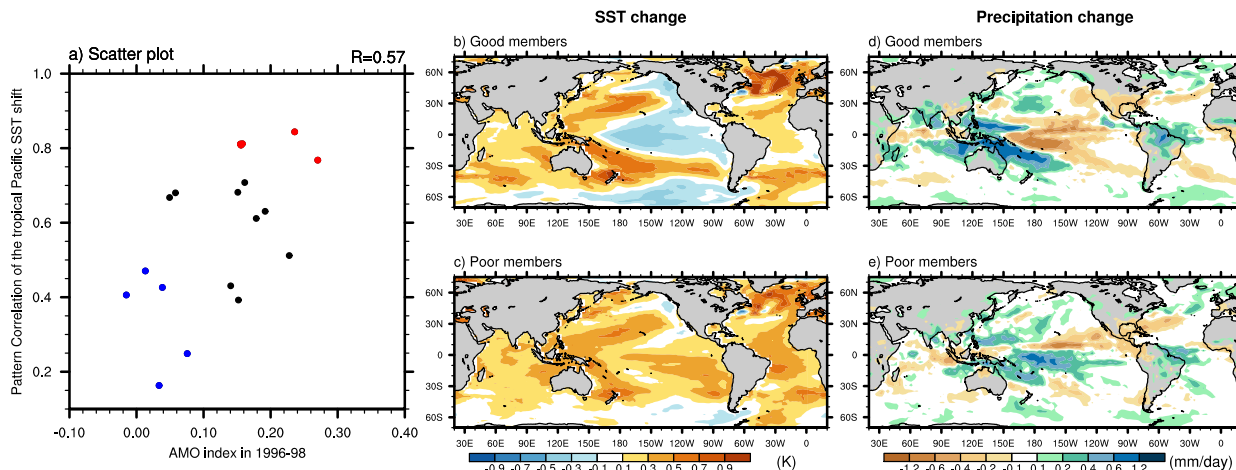


**Figure 2.** (a) Scatter diagram of each ensemble member in the initialized simulation for the AMO index in 1996–98 and the predictive skill of SST shift in the tropical Pacific. The AMO index is based on the definition by *Trenberth and Shea* [2006]. The predictive skill is estimated by the pattern correlation coefficient of SST shift (the 2000–04 mean minus the 1991–95 mean) between the observations and initialized simulation ( $35^{\circ}\text{S}$ – $35^{\circ}\text{N}$ ). Note that there is a time lag between the AMO index and the pattern correlation coefficient of SST shift. Red and blue marks indicate the good and poor members, respectively. Right two panels show SST and precipitation changes from 1991–95 to 2000–04 in (b, d) good and (c, e) poor members.

the amplitude of the SST change in the Pacific region is relatively smaller than that in the observation. In addition to this SST change pattern, the zonal precipitation gradient appears over the tropical Pacific and Atlantic regions in the initialized simulation: the suppressed precipitation in the central to eastern tropical Pacific and the enhanced precipitation in the western tropical Pacific and the tropical Atlantic (Fig. 1b). On the other hand, the uninitialized simulation tends to show a uniform zonal change in SST and precipitation (Figs. 1c, f), indicating a strengthened Hadley circulation in the tropical Pacific associated with the externally forced component. These results suggest that initialization is important to simulate the stepwise climate change in the Pacific and Atlantic during the 1990s.

From 1997 to 1998, two years after the AMO phase change, a stepwise change appeared in the western subtropical Pacific SST (Fig. S2). This lag relationship suggests that the AMO may be able to affect the predictability of the SST shift pattern in the Pacific through the tropical linkage of zonal circulation between the Pacific and Atlantic [*Zhang and Delworth*, 2007; *Kucharski et al.*, 2011]. Figure 2a shows a scatter plot of the AMO index during the 1996–98 period and the pattern correlation coefficient of the SST shift pattern from 1991–95 to 2000–04 between the observations and the initialized simulation for each ensemble member. Higher values of pattern correlation coefficient indicate that the observed SST shift pattern in the tropical Pacific is simulated well by that ensemble member in the initialized simulation, implying higher predictability in the Pacific stepwise shift during the 1990s. The scatter plot between the AMO index and the predictability of the following SST shift pattern in the tropical Pacific shows significant positive correlation (correlation coefficient  $R = 0.57$ ). This positive correlation coefficient indicates that members with large positive value of AMO index during the 1996–98 period show good agreement with the observed SST shift pattern in the tropical Pacific and vice versa. In fact, a comparison of good members with higher AMO index and SST predictability (five higher members) clearly shows the La Niña-like SST pattern in the Pacific (Fig. 2b), while that with poor members (five lower members) show a warming of SST in the eastern tropical Pacific (Fig. 2c). Moreover, the good members simulation shows the enhanced precipitation in the tropical Atlantic and the strengthened Pacific Walker circulation

(Figs. 2d, e). This relationship between the AMO index and the Pacific SST predictability is also confirmed in the decadal prediction experiment of the CMIP5 models (Fig. S3). Although the Pacific ENSO has a strong impact on the Atlantic climate variability, particularly, on interannual timescales [*Chikamoto and Tanimoto*, 2005], our results suggest that the AMO has a significant effect on the Pacific SST variability on decadal timescales through changes in the Walker circulation.

#### 4. Discussion

We suggest a possible process through which the AMO can affect the stepwise climate change in the Pacific through the zonal circulation in the tropics as follows. Around 1995, an abrupt phase change in AMO index from negative to positive occurred, which was associated with the phase change of NAO [*Robson et al.*, 2012]. Because a positive phase of AMO accompanies positive SST anomalies in the entire North Atlantic basin except for the western mid-latitude region, SST warming also occurred in the northern tropical Atlantic around 1995. This SST warming induced a zonal SST gradient in the northern subtropics between the Atlantic and Pacific, which accompanied the enhanced precipitation and the wind divergence in the upper troposphere over the tropical Atlantic. In fact, observations during the 1955–2010 period show that the AMO index was significantly correlated ( $R = 0.70$ ) with the zonal SST gradient in the northern subtropics between the Atlantic ( $5^{\circ}\text{N}$ – $15^{\circ}\text{N}$ ,  $60^{\circ}\text{W}$ – $30^{\circ}\text{W}$ ) and Pacific regions ( $5^{\circ}\text{N}$ – $15^{\circ}\text{N}$ ,  $150^{\circ}\text{W}$ – $90^{\circ}\text{W}$ ) (Fig. 3a). Moreover, in both the MIROC and CMIP5 models, members with higher predictability of stepwise SST change in the tropical Pacific show a larger zonal SST gradient between the Atlantic and Pacific (Fig. S4); the correlation coefficient with the Pacific SST predictability becomes higher against the zonal SST gradient ( $R = 0.65$  in MIROC and  $0.37$  in the CMIP5 multi-model ensemble) than the AMO index ( $R = 0.57$  and  $0.32$ ). Associated with the zonal SST gradient, the Atlantic wind divergence in the upper troposphere can induce the strong subsidence in the eastern tropical Pacific, and then contribute to the strengthened Pacific Walker circulation. As a result, the SST change in the tropical Pacific

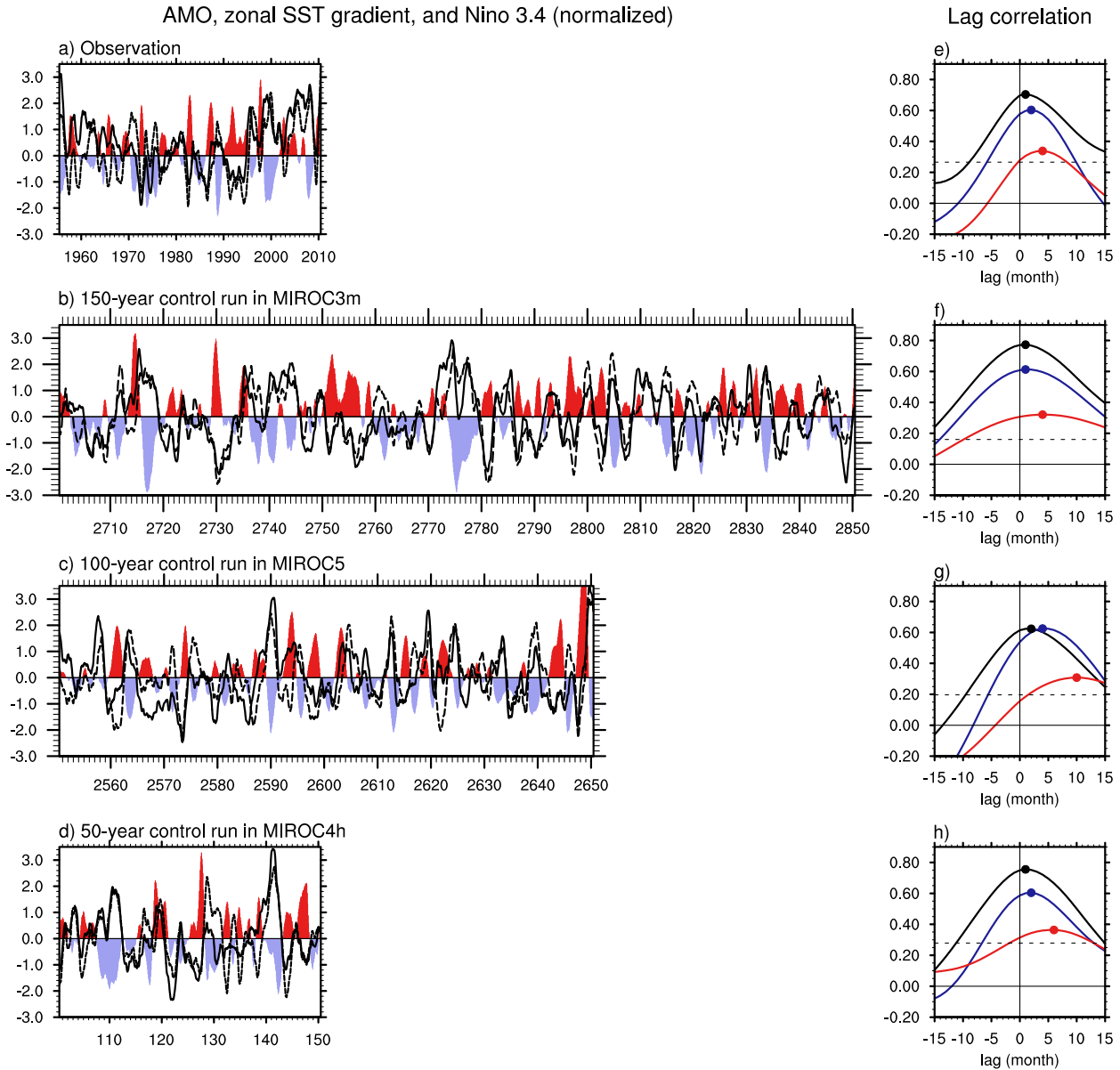


**Figure 3.** Time series of the AMO index (solid line), a zonal SST gradient (broken line) in the northern subtropics between the Atlantic ( $5^{\circ}\text{N}$ – $15^{\circ}\text{N}$ ,  $60^{\circ}\text{W}$ – $30^{\circ}\text{W}$ ) and Pacific regions ( $5^{\circ}\text{N}$ – $15^{\circ}\text{N}$ ,  $150^{\circ}\text{W}$ – $90^{\circ}\text{W}$ ), and Niño 3.4 index (bars) in (a) observation for 1955–2010 and in pre-industrial control simulations of (b) MIROC3m for 150 years, (c) MIROC5 for 100 years, and (d) MIROC4h for 50 years. All indices are normalized by one standard deviation and applied by a 12-month running mean filtering. Right panels indicate lag correlation coefficients between the AMO and zonal SST gradient indices (black), the zonal SST gradient and Niño 3.4 indices (blue and reversed sign), and the AMO and Niño 3.4 indices (red and reversed sign) in (e) observation and control simulations of (f) MIROC3m, (g) MIROC5, and (h) MIROC4h. Maximum correlation coefficient is denoted by a circle. A positive lag indicates a AMO lead or a Niño 3.4 lag. Dotted line in the right panels corresponds to statistical significance at the 95% level using a two-sided Student *t*-test with 53, 148, 98, and 48 degrees of freedom in observation, MIROC3m, MIROC5, and MIROC4h, respectively.

will show the La Niña-like pattern on decadal timescales through an air-sea coupling process.

The process influencing from AMO to the tropical Pacific climate is also confirmed by a lag correlation analysis. Figure 3 shows time series and lag correlation coefficients among the AMO, zonal SST gradient, and Niño 3.4 indices in observation and the pre-industrial control simulation in three versions of MIROC. In the observation for the 1955–2010 period, the AMO index has a maximum correlation coefficient of  $-0.34$  with the Niño 3.4 index at a 4-month lag. This re-

lationship is improved by taking the zonal SST gradient into account: the zonal SST gradient is correlated with the AMO index at a 1-month lead ( $R = 0.70$ ) and the Niño 3.4 index at a 2-month lag ( $R = -0.60$ ). These significant correlation coefficients among three indices also appear in pre-industrial control simulations of three versions of MIROC (Fig. 3). In other words, the AMO can affect the ENSO phase through internal variability on decadal timescales. While the precise timing of phase change such as AMO and ENSO is hard to predict on interannual timescales, we would be able to pre-



dict a decadal climate change pattern by improving a model and initialization techniques.

## 5. Conclusion

We investigated the relationship between changes in the Pacific and Atlantic climate during the 1990s using the decadal climate prediction experiments conducted by three versions of the MIROC and CMIP5 models. Observations from the early 1990s to the early 2000s show a SST warming in the North Atlantic and a La Niña-like SST pattern in the Pacific. Associated with these SST pattern changes, the observations indicate enhanced precipitation in the tropical Atlantic and a strengthened Walker circulation in the tropical Pacific. These observed changes in SST and precipitation are simulated well in the initialized simulations but are poorly simulated in the uninitialized simulations. In the initialized simulations, particularly, ensemble members with larger amplitude of AMO index during the 1996–98 period tend to capture the observed shifted SST pattern in the tropical Pacific better. Our results suggest that the ocean initialization not only in the Pacific but also in the North Atlantic plays an important role for the predictability of the Pacific stepwise change during the late 1990s.

In nature, abrupt climate change is observed as a combination of internally generated and externally forced variations. Surface temperature anomalies induced by increased carbon dioxide concentration, the main part of the externally forced component, have an upward trend while internally generated variabilities like PDO, IPO, or AMO contribute to both positive and negative temperature anomalies. Therefore, the upward trend of surface air temperature under the global warming seems to be weakened during the cooling phase of the internally generated variability, but seem to be strengthened during its warming phase [Meehl *et al.*, 2009]. In terms of the late 1990s climate change, the uninitialized simulations overestimate the observed global temperature change, while the initialized simulations, particularly in good member experiments, provide an accurate estimation of the change due to a more realistic simulation of La Niña-like changes in the tropical Pacific (Fig. S5). The prediction of these climate changes would be useful for forecasting not only atmospheric phenomena such as typhoon frequency and Asian monsoon variability but also marine fisheries factors such as fish production and stock in the coming decade.

**Acknowledgments.** The manuscript benefited from the constructive comments of two anonymous reviewers. This study was supported by the Japanese Ministry of Education, Culture, Sports, Science and Technology through the Innovative Program of Climate Change Projection for the twenty-first Century. The simulations were performed with the Earth Simulator at the Japan Agency for Marine Earth Science and Technology and the NEC SX-8R at the National Institute for Environmental Studies, Japan.

## References

- Bloom, S. C., L. Takacs, A. M. da Silva, and D. Ledvina (1996), Data assimilation using incremental analysis updates, *Mon. Wea. Rev.*, *124*, 1256–1271.
- Chikamoto, Y., and Y. Tanimoto (2005), Role of specific humidity anomalies in Caribbean SST response to ENSO, *J. Meteorol. Soc. Japan*, *83*, 959–975.
- Chikamoto, Y., et al. (2012a), Predictability of a stepwise shift in Pacific climate during the late 1990s in hindcast experiments using MIROC, *J. Meteorol. Soc. Japan*, *90A*, 1–21, doi:10.2151/jmsj.2012-A01.
- Chikamoto, Y., et al. (2012b), An overview of decadal climate predictability in a multi-model ensemble by climate model miroc, *Climate Dyn.*, doi:10.1007/s00382-012-1351-y.
- Ishii, M., and M. Kimoto (2009), Reevaluation of historical ocean heat content variations with time-varying XBT and MBT depth bias corrections, *J. Oceanogr.*, *65*(3), 287–299.
- Kajikawa, Y., and B. Wang (2012), Interdecadal change of the south china sea summer monsoon onset, *J. Climate*, *25*, 3207–3218.
- Keenlyside, N. S., M. Latif, J. Jungclauss, L. Kornblueh, and E. Roeckner (2008), Advancing decadal-scale climate prediction in the north atlantic sector, *Nature*, *453*, 84–88, doi:10.1038/nature06921.
- Kim, W.-M., J.-G. Jhun, K.-J. Ha, and M. Kimoto (2011), Decadal changes in climatological intraseasonal fluctuation of subseasonal evolution of summer precipitation over the Korean peninsula in mid-1990s, *Adv. Atmos. Sci.*, *28*(3), 591–600.
- Knight, J., R. Allan, C. Folland, M. Vellinga, and M. Mann (2005), A signature of persistent natural thermohaline circulation cycles in observed climate, *Geophys. Res. Lett.*, *32*, L20,708.
- Kucharski, F., I. Kang, R. Farneti, and L. Feudale (2011), Tropical pacific response to 20th century atlantic warming, *Geophys. Res. Lett.*, *38*, L03,702.
- Mantua, N. J., and S. R. Hare (2002), The pacific decadal oscillation, *J. Oceanogr.*, *58*, 35–44.
- Mantua, N. J., S. R. Hare, Y. Zhang, J. M. Wallace, and R. C. Francis (1997), A Pacific interdecadal climate oscillation with impacts on salmon production, *Bull. Amer. Meteorol. Soc.*, *78*, 1069–1079.
- Meehl, G. A., A. Hu, and B. D. Santer (2009), The mid-1970s climate shift in the pacific and the relative roles of forced versus inherent decadal variability, *J. Climate*, *22*(3), 780–792.
- Mochizuki, T., et al. (2010), Pacific decadal oscillation hindcasts relevant to near-term climate prediction, *Proc. Natl. Acad. Sci. USA*, *107*, 1833, doi:10.1073/pnas.0906531107.
- Mochizuki, T., Y. Chikamoto, M. Kimoto, M. Ishii, H. Tatebe, Y. Komuro, T. T. Sakamoto, M. Watanabe, and M. Mori (2012), Decadal prediction using a recent series of MIROC global climate models, *J. Meteorol. Soc. Japan, Special Issue*, *90A*, 373–383.
- Nozawa, T., T. Nagashima, T. Ogura, T. Yokohata, N. Okada, and H. Shioyama (2007), Climate change simulations with a coupled ocean-atmosphere GCM called the model for interdisciplinary research on climate: MIROC, *CGER Supercomput. Monogr. Rep.*, *12*, cent. for Global Environ. Res., Natl. Inst. for Environ. Stud., Tsukuba, Japan.
- Reverdin, G. (2010), North Atlantic subpolar gyre surface variability (1895–2009), *J. Climate*, *23*(17), 4571–4584.
- Robson, J., R. Sutton, K. Lohmann, D. Smith, and M. D. Palmer (2012), Causes of the rapid warming of the North Atlantic Ocean in the mid 1990s, *J. Climate*, *25*, 4116–4134, doi:10.1175/JCLI-D-11-00443.1.
- Sakamoto, T. T., et al. (2012), MIROC4h - a new high-resolution atmosphere-ocean coupled general circulation model, *J. Meteorol. Soc. Japan*, *90*, 325–359, doi:10.2151/jmsj.2012-301.
- Smith, D., R. Eade, N. Dunstone, D. Fereday, J. Murphy, H. Pohlmann, and A. Scaife (2010), Skilful multi-year predictions of Atlantic hurricane frequency, *Nature geoscience*, *3*, 846–849.
- Sutton, R. T., and D. L. R. Hodson (2005), Atlantic ocean forcing of North American and European summer climate, *Science*, *309*(5731), 115.
- Tatebe, H., et al. (2012), The initialization of the MIROC climate models with hydrographic data assimilation for decadal prediction, *J. Meteorol. Soc. Japan, Special Issue*, *90A*, 275–294.
- Trenberth, K. E., and D. J. Shea (2006), Atlantic hurricanes and natural variability in 2005, *Geophys. Res. Lett.*, *33*(12), L12,704.
- Tu, J., C. Chou, and P. Chu (2009), The abrupt shift of typhoon activity in the vicinity of Taiwan and its association with western North Pacific-East Asian climate change, *J. Climate*, *22*(13), 3617–3628.
- Watanabe, M., et al. (2010), Improved climate simulation by MIROC5: Mean states, variability, and climate sensitivity, *J. Climate*, *23*(23), 6312–6335, doi:10.1175/2010JCLI3679.1.

Zhang, R., and T. L. Delworth (2007), Impact of the atlantic multidecadal oscillation on north pacific climate variability, *Geophys. Res. Lett.*, *34*(23), L23,708.

of Ocean Earth Science and Technology, University of Hawaii at Manoa, 1680 East-West Road, Honolulu, HI, 96822, USA.

---

Y. Chikamoto, International Pacific Research Center, School (chika44@hawaii.edu)

## Climate change from 1991/95 to 2000/04 (OBS)

## Divergent wind

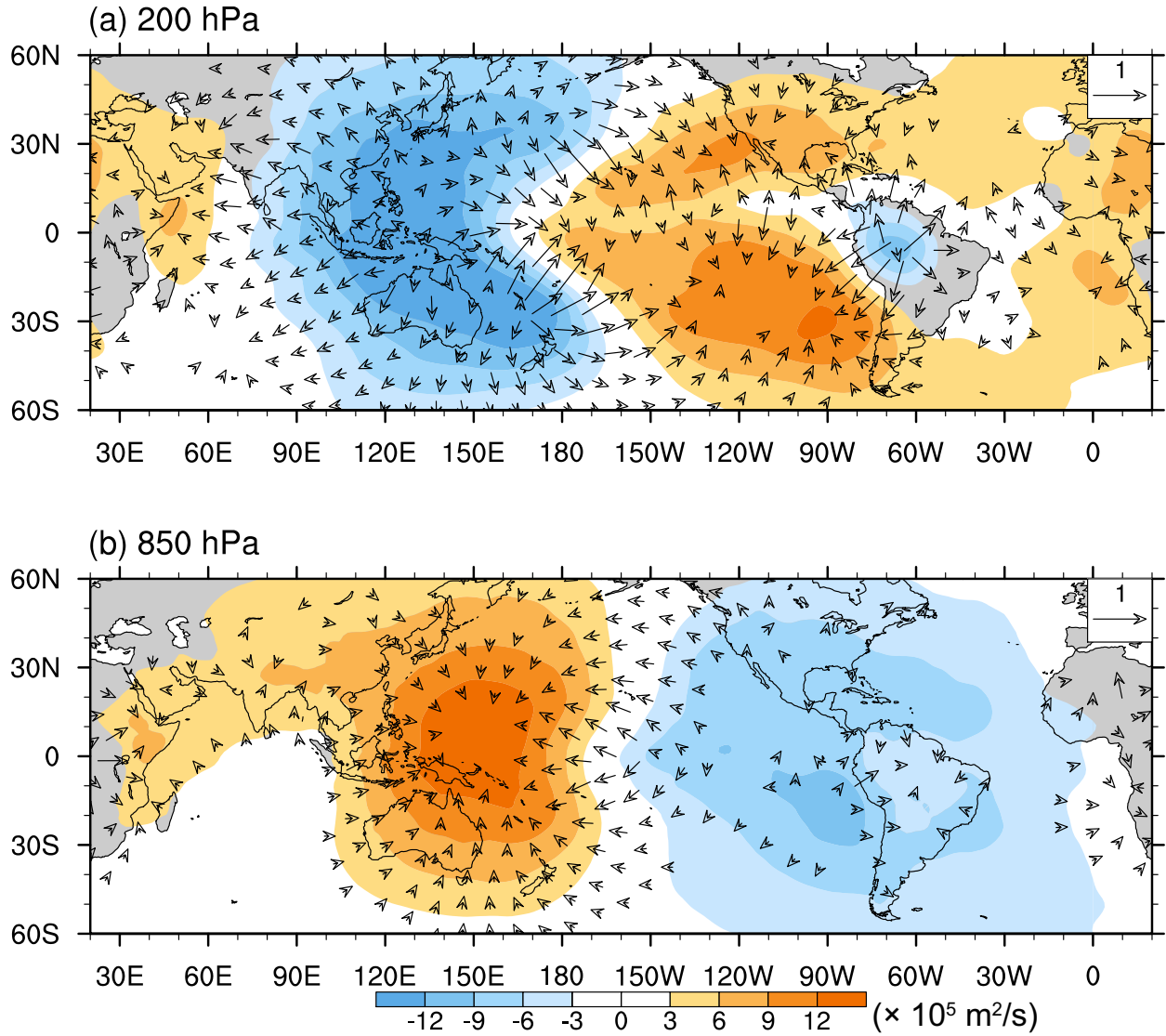


**Figure S1.** Observed decadal change of divergent wind at (a) 200 and (b) 850 hPa from 1991-95 to 2000-04. Contours and vectors indicate velocity potential (contour interval: 300000  $\text{m}^2/\text{s}$ ) and divergent wind component (reference vector in upper-right corner: 1  $\text{m/s}$ ), respectively.

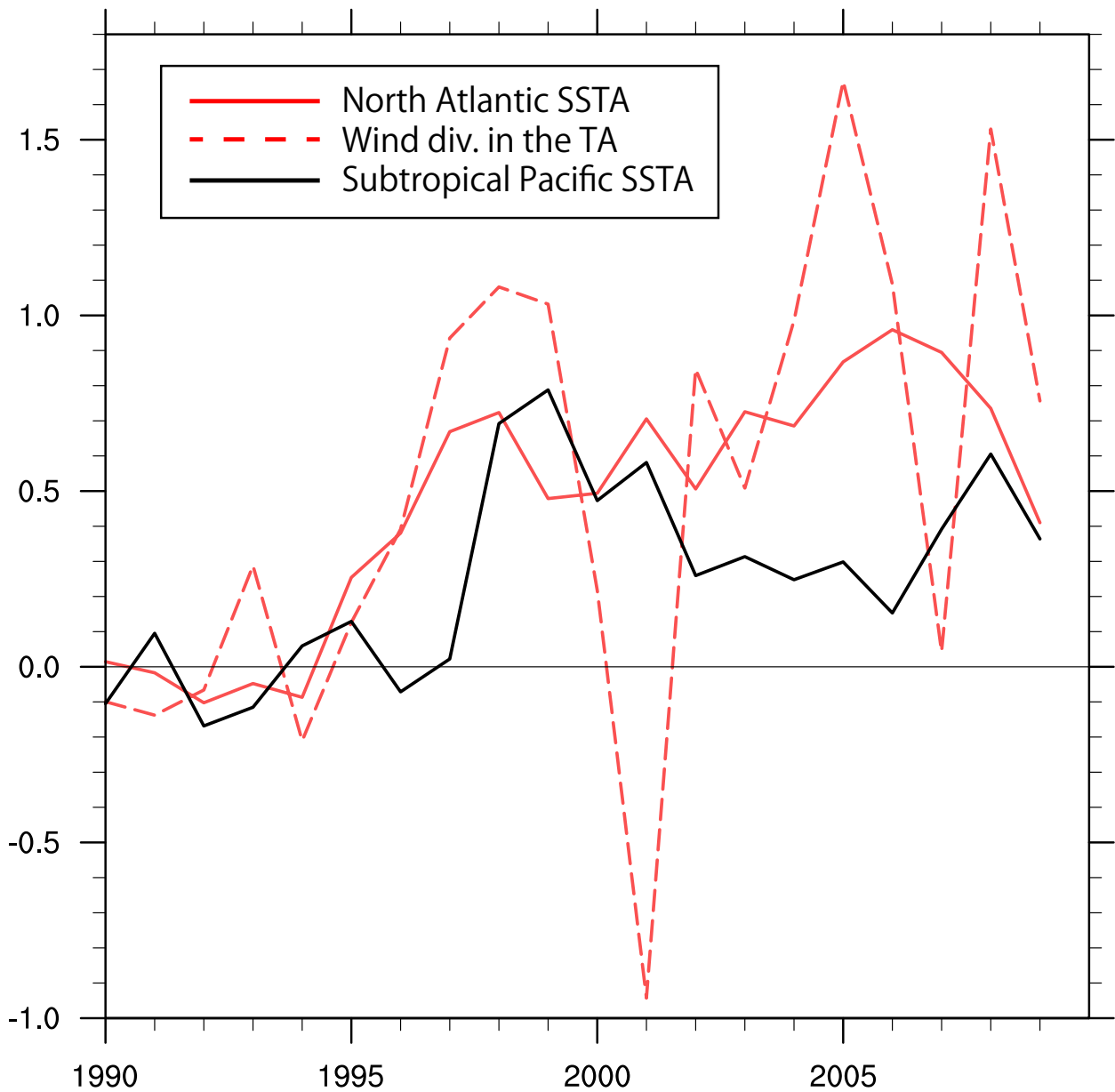


**Figure S2.** Time series of observed SST anomalies in the North Atlantic (red solid line: 45N-70N, 60W-0), the western subtropical Pacific (black solid line: 15N-30N, 130E-160E), and velocity potential anomalies at 200 hPa in the tropical Atlantic (red broken line: 70W-30W, 10S-10N) in observation. The velocity potential anomalies are scaled down by a factor of 1000000 and their sign reversed.



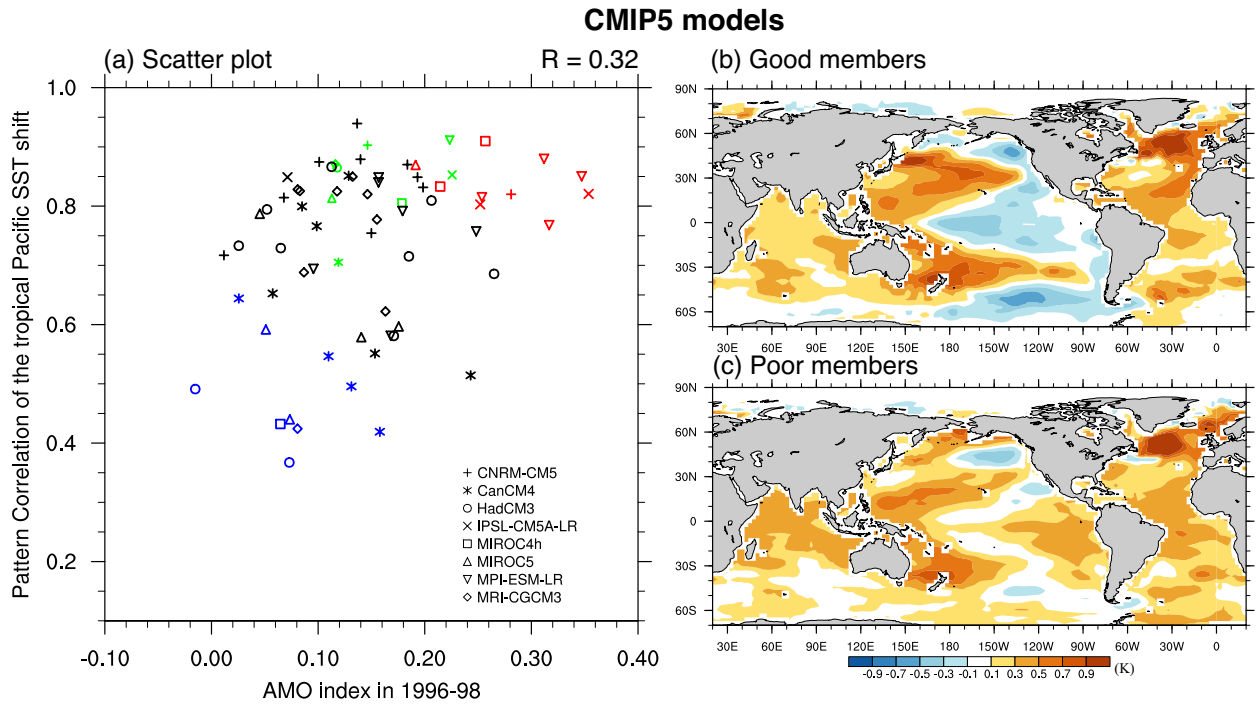


**Figure S3.** Same as Fig. 2 but for ensemble members of the CMIP5 models. Green marks indicate the ensemble mean for each CMIP5 model. Note that there is a time lag between the AMO index and the pattern correlation coefficient of SST shift.

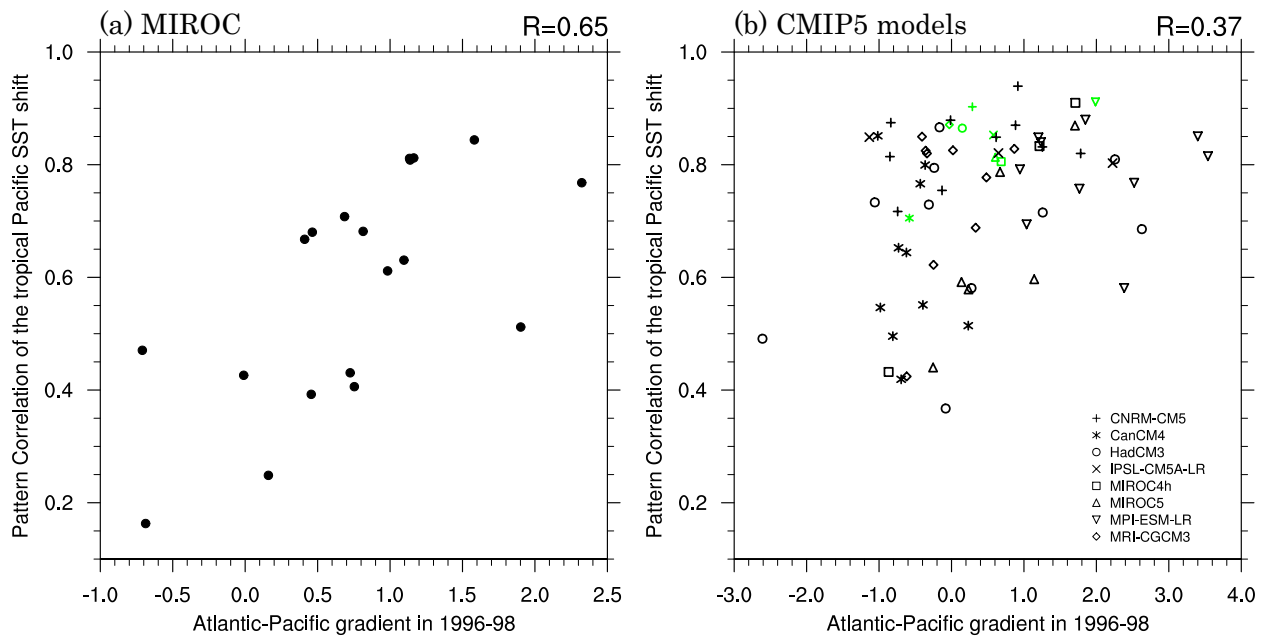


**Figure S4.** Same as Figs. 2a and S3a, but for the zonal SST gradient in the northern subtropics between the Atlantic (5N-15N, 60W-30W) and Pacific regions (5N-15N, 150W-90W) in 1996-98. The zonal SST gradient is normalized by an annual-mean standard deviation for the 1996-2005 period, based on the assimilation in MIROC and the ensemble mean of each model in CMIP5. Note that there is a time lag between the zonal SST gradient and the pattern correlation coefficient of SST shift.

## Climate change in surface air temperature

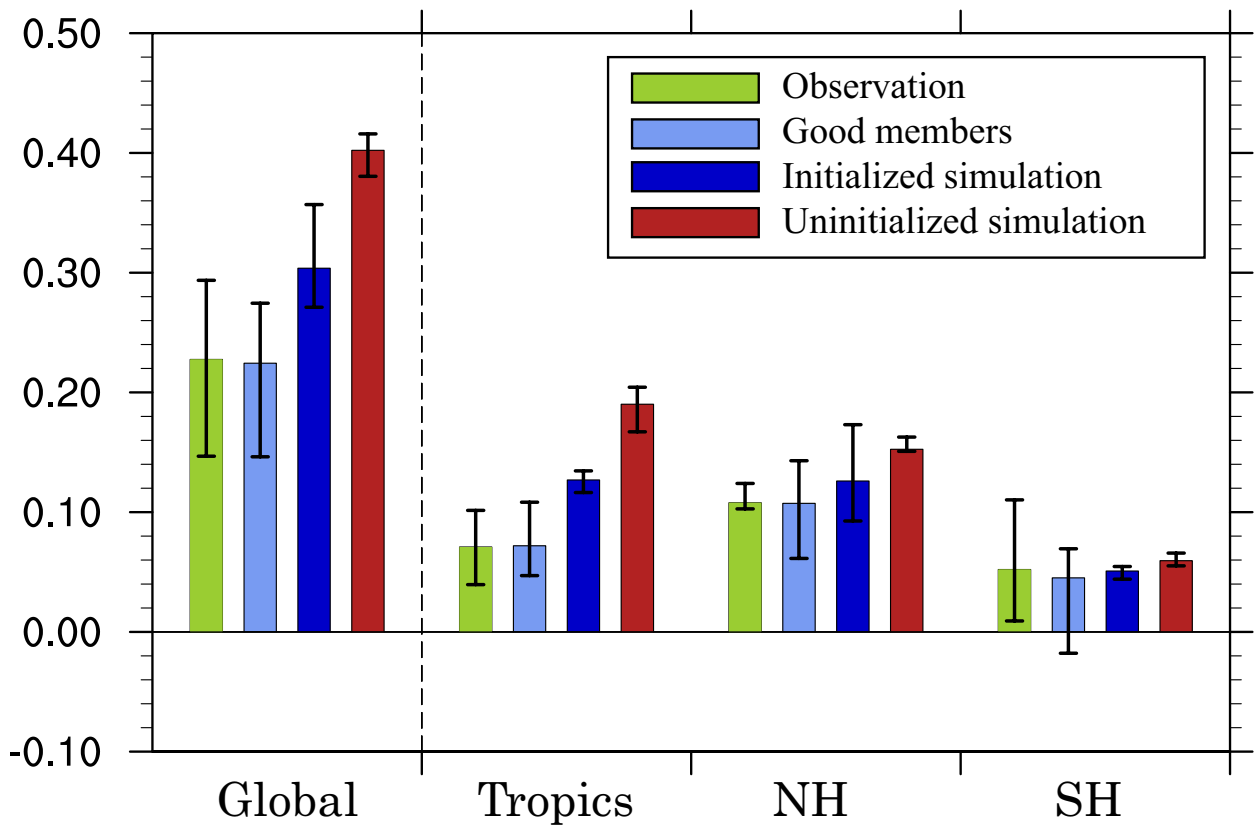


**Figure S5.** Climate changes in surface air temperature from 1991-95 to 2000-04, averaged over the global region, tropics (30S-30N), northern extra-tropics (30N-90N), and southern extra-tropics (90S-30S). Green, light blue, dark blue, and red boxes indicate means in the observation (ERA Interim, NCEP, NCEP2, JRA, and HadCRU), good members in the initialized simulation, good members in the initialized simulation, and the initialized and uninitialized simulations in the MIROC multi-model, respectively. Error bars indicate a maximum-to-minimum range in observations, good members, and ensemble means in three versions of MIROC.